Chapter 6

Comparison of Modelling Approaches

6.1 Introduction

In order to model the frequency dependant behaviour of the sound absorption two models were adopted to predict the acoustic performance of the extruded materials made from polymeric waste, the Pade approximation model (1998), and the Johnson Champoux Allard model (1991). A summary of these models is given in Table 6.1. The Pade approximation model is based entirely on a set of four measurable non-acoustic parameters, which are the porosity, flow resistivity, tortuosity and the standard deviation. It will be shown that this model is able to provide a very close fit to the measured data for materials made from recycled polymeric waste. The Johnson-Champoux-Allard model is based on three measurable (M) and two adjustable (A) non-acoustical parameters: porosity (M), flow resistivity (M), tortuosity (M), viscous characteristic length (A) and thermal characteristic length (A). The details of these two models are given in chapter 4.

Table 6.1: Summary of two models to predict the acoustic performance

Model	Type	Parameters required
Pade approximation	Analytical	Flow resistivity, porosity, tortousity, standard deviation and thickness.
Johnson-Champoux-Allard	Analytical	Flow resistivity, porosity, tortousity, viscous characteristic length, thermal characteristic length, and thickness.

The predicted and measured acoustic properties of rigid frame porous media which were adopted for the investigation will be presented in this section. Figures showing agreement between the experimental values of the absorption coefficient and those predicted by the Pade approximation and by the Johnson-Champoux-Allard model are presented below. The following tables present the measured and inverted values of the related non-acoustical parameters which were used to predict the observed acoustical absorption behaviour of the developed samples.

6.2 Pade Approximation Approach

Figures 6.1 – 6.5 and Tables 6.2 – 6.6 present the data associated with modelling with the Pade approximation approach. Some values of the non-acoustical parameters had to be adjusted to improve the fit between the measured and predicted data.

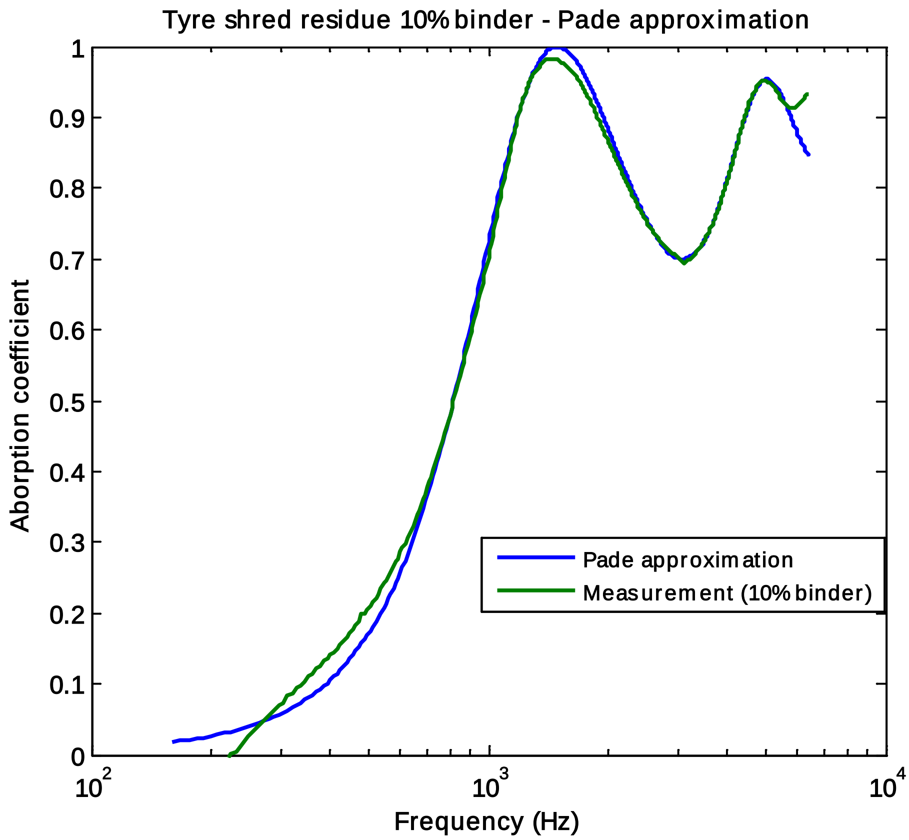

Figure 6.1: Pade approximation for 10% binder level

Table 6.2: Summary of the parameters used in Pade approximation for 10% binder

Material	**Binder (%)**	**Resistivity (N.s/m^4)**	**Porosity (%)**	**Tortuosity**	**Stand dev.**	**Thickness (mm)**
Rayon (original)	10	10,200	67	1.4	-	32
Rayon (adjusted)	10	10,200 (0%)	70 (4%)	1.5 (7%)	0.4	31(3%)

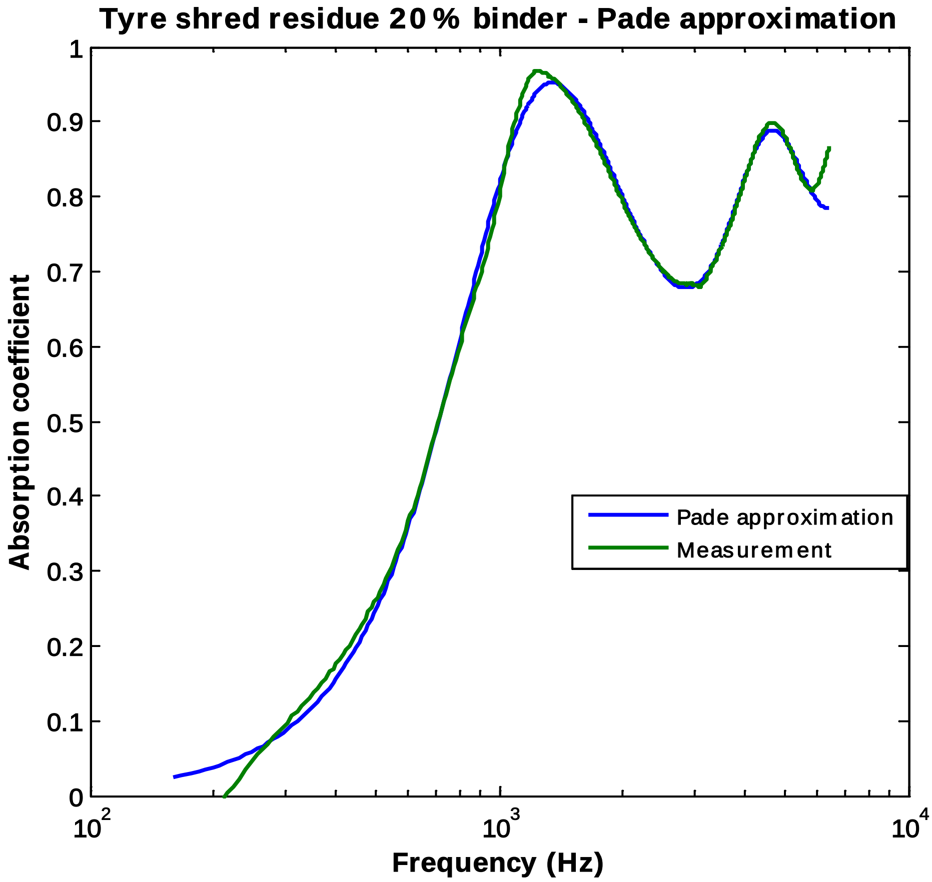

Figure 6.2: Pade approximation for 20% binder level

Table 6.3: Summary of the parameters used in Pade approximation for 20% binder

Material	**Binder (%)**	**Resistivity ($N.s/m^4$)**	**Porosity (%)**	**Tortuosity**	**Stand dev.**	**Thickness (mm)**
Rayon (original)	20	9,100	71	1.6	-	33
Rayon (adjusted)	20	9,100 (0%)	72(1%)	1.8(12%)	0.4	32(-3%)

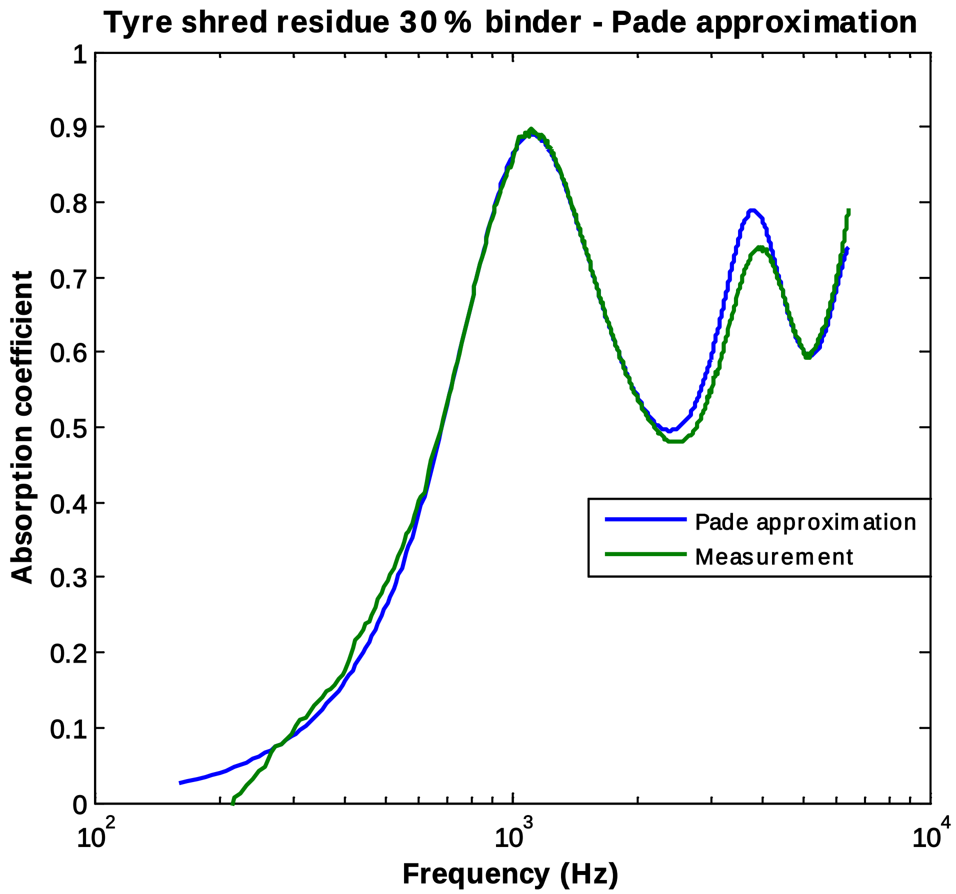

Figure 6.3: Pade approximation for 30% binder level

Table 6.4: Summary of the parameters used in Pade approximation for 30% binder

Material	Binder (%)	Resistivity (N.s/m^4)	Porosity (%)	Tortuosity	Stand dev.	Thickness (mm)
Rayon(original)	30	8,900	72	1.6	-	30
Rayon(adjusted)	30	8,900(0%)	73(1%)	1.7(6%)	0.4	33(10%)

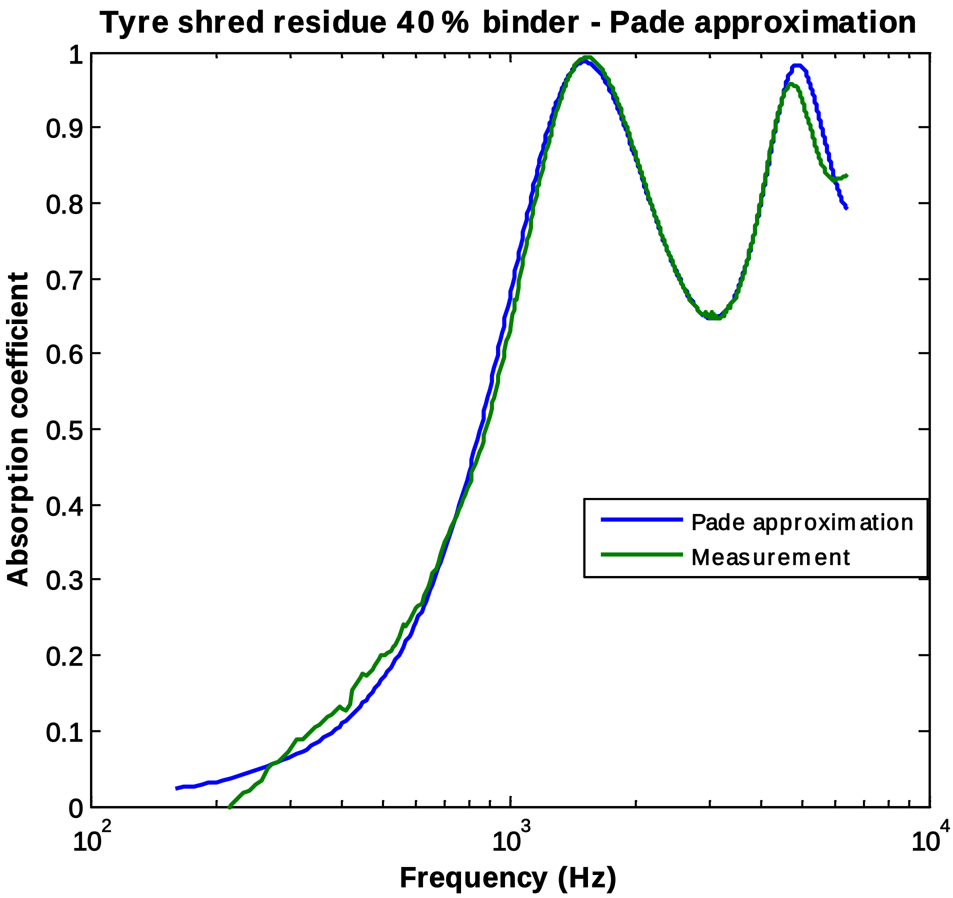

Figure 6.4: Pade approximation for 40% binder level

Table 6.5: Summary of the parameters used in Pade approximation for 40% binder

Material	Binder (%)	Resistivity (N.s/m^4)	Porosity (%)	Tortuosity	Stand dev.	Thickness (mm)
Rayon(original)	40	8600	77	1.7	-	32
Rayon(adjusted)	40	8,900(3%)	78(1%)	1.6(-6%)	0.4	32(0%)

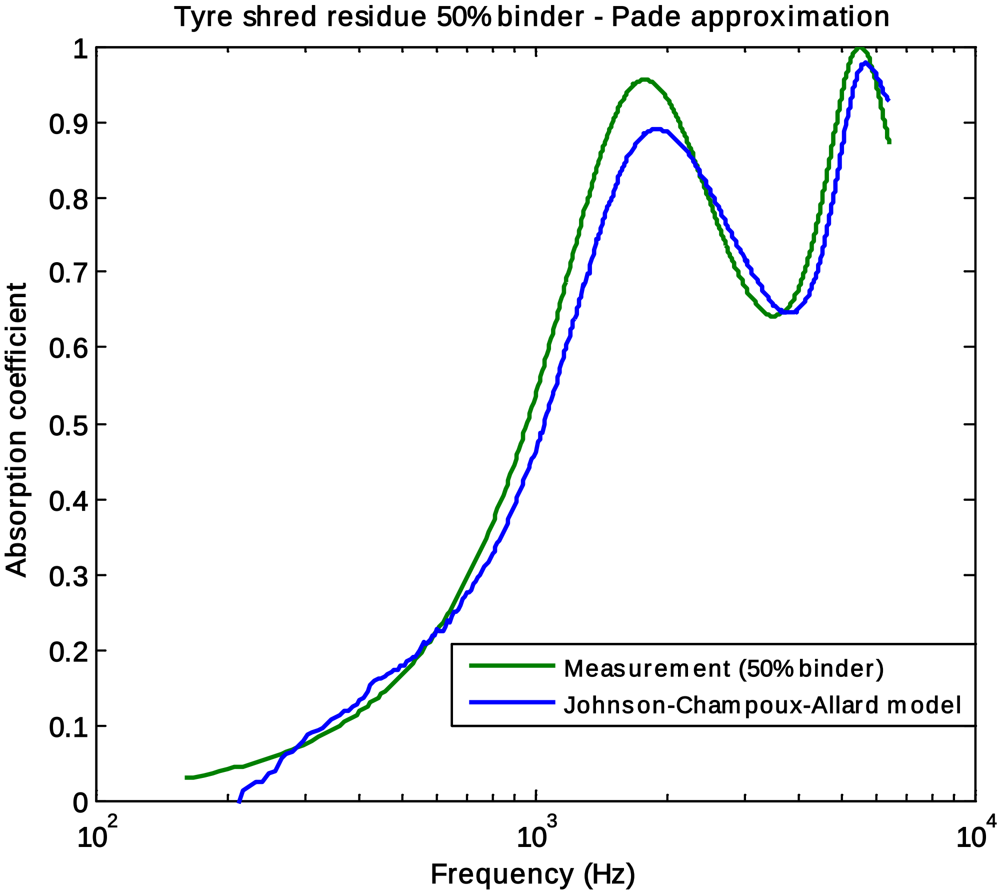

Figure 6.5: Pade approximation for 50% binder level

Table 6.6: Summary of the parameters used in Pade approximation

Material	Binder (%)	Resistivity ($N.s/m^4$)	Porosity (%)	Tortuosity	Stand dev.	Thickness (mm)
Rayon (original)	50	8,050	89.6	1.7	-	30
Rayon (adjusted)	50	8,000(1%)	77(-14%)	1.6(6%)	0.4	33(10%)

The adjusted values of the parameters have been used in these calculations shown in Tables 6.2 to 6.6. The value of porosity requires a considerable adjustment in some cases, as high as 14%. This can be considered unrealistic as this value is easy to measure using the method detailed in chapter 4.

6.3 Johnson-Champoux-Allard Approach

Figures 6.6 – 6.10 and Table 6.7 – 6.11 present the data associated with modelling with the Johnson-Champoux-Allard approach.

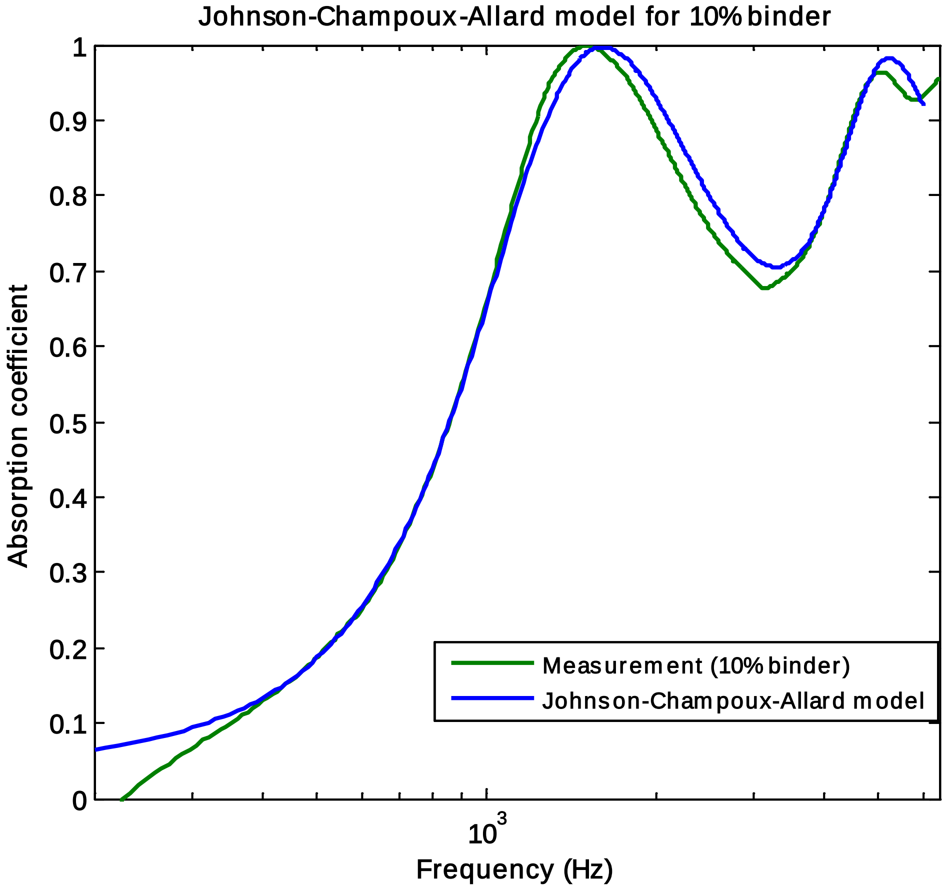

Figure 6.6: Johnson-Champoux-Allard model for 10% binder level

Table 6.7: Summary of the parameters used in the Johnson-Champoux-Allard model for 10% binder

Material	Binder (%)	Resistivity (N.s/m^4)	Porosity (%)	Tortuosity	Λ (μm)	Λ' (μm)	Thickness (mm)
Rayon (original)	10	10,200	67	1.4	-	-	32
Rayon (adjusted)	10	9,500 (-7%)	69 (3%)	1.8 (28%)	60	50	30(-6%)

In particular cases the value of the tortuosity requires a considerable increase of 28% (Table 5.15). This can be a result from the high density of the sample made using 10 % binder.

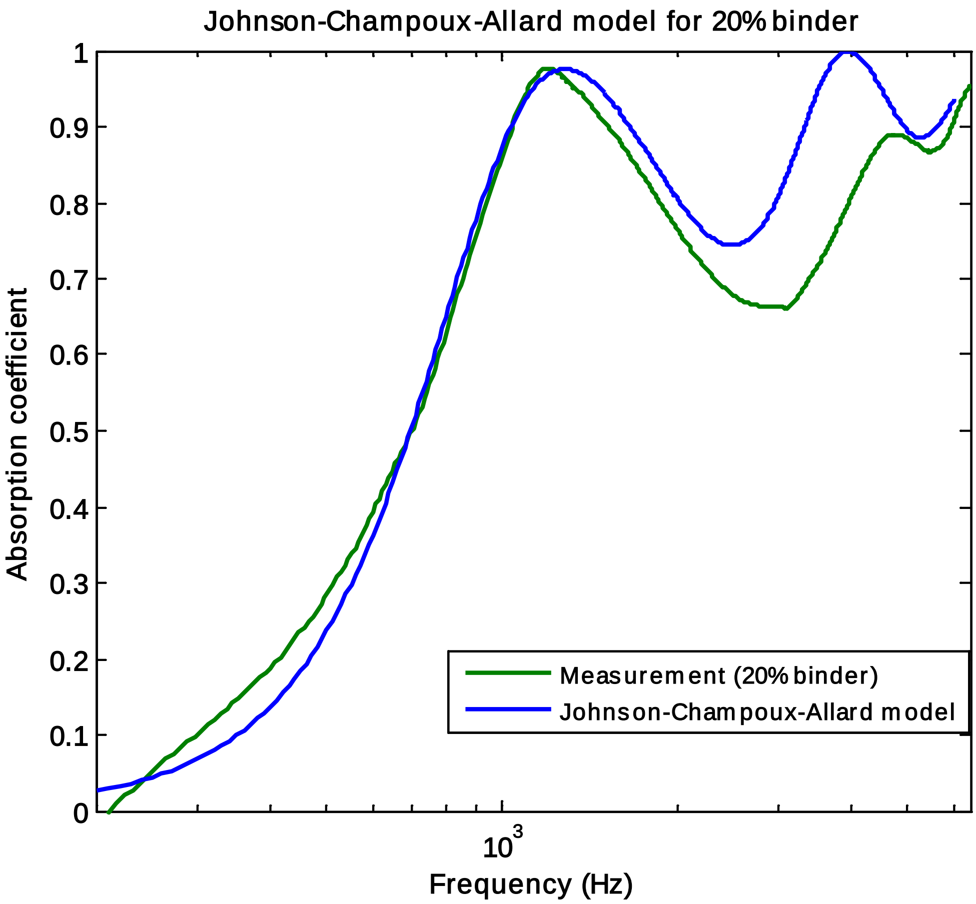

Figure 6.7: Johnson-Champoux-Allard model for 20% binder level

Table 6.8: Summary of the parameters used in the Johnson-Champoux-Allard model for 20% binder

Material	Binder (%)	Resistivity (N.s/m^4)	Porosity (%)	Tortuosity	Λ (μm)	Λ' (μm)	Thickness (mm)
Rayon (original)	20	9,100	71	1.6	-	-	32
Rayon (adjusted)	20	8,445(-7%)	74(4%)	1.8(12%)	75	20	30(-6%)

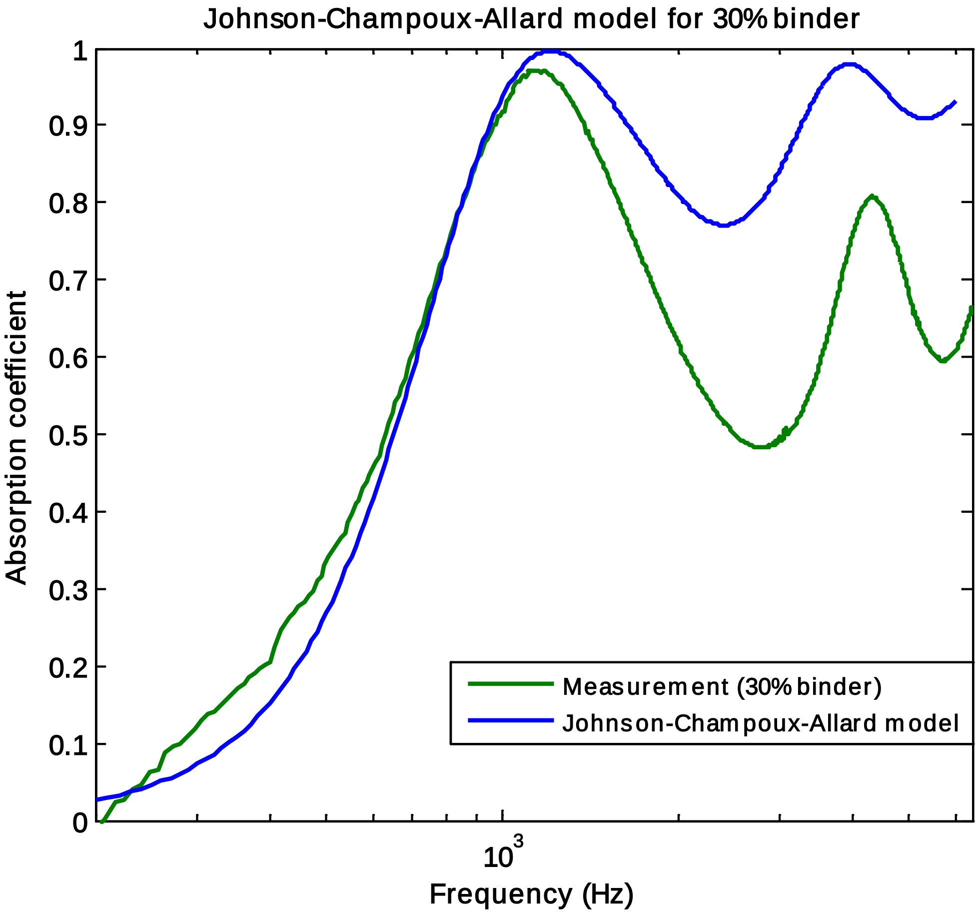

Figure 6.8: Johnson-Champoux-Allard model for 30% binder level

Table 6.9: Summary of the parameters used in the Johnson-Champoux-Allard model for 30% binder

Material	Binder (%)	Resistivity (N.s/m^4)	Porosity (%)	Tortuosity	Λ (μm)	Λ' (μm)	Thickness (mm)
Rayon(original)	30	8,900	72	1.6	-	-	30
Rayon(adjusted)	30	8,950(1%)	73(1%)	1.7(6%)	55	40	30(0%)

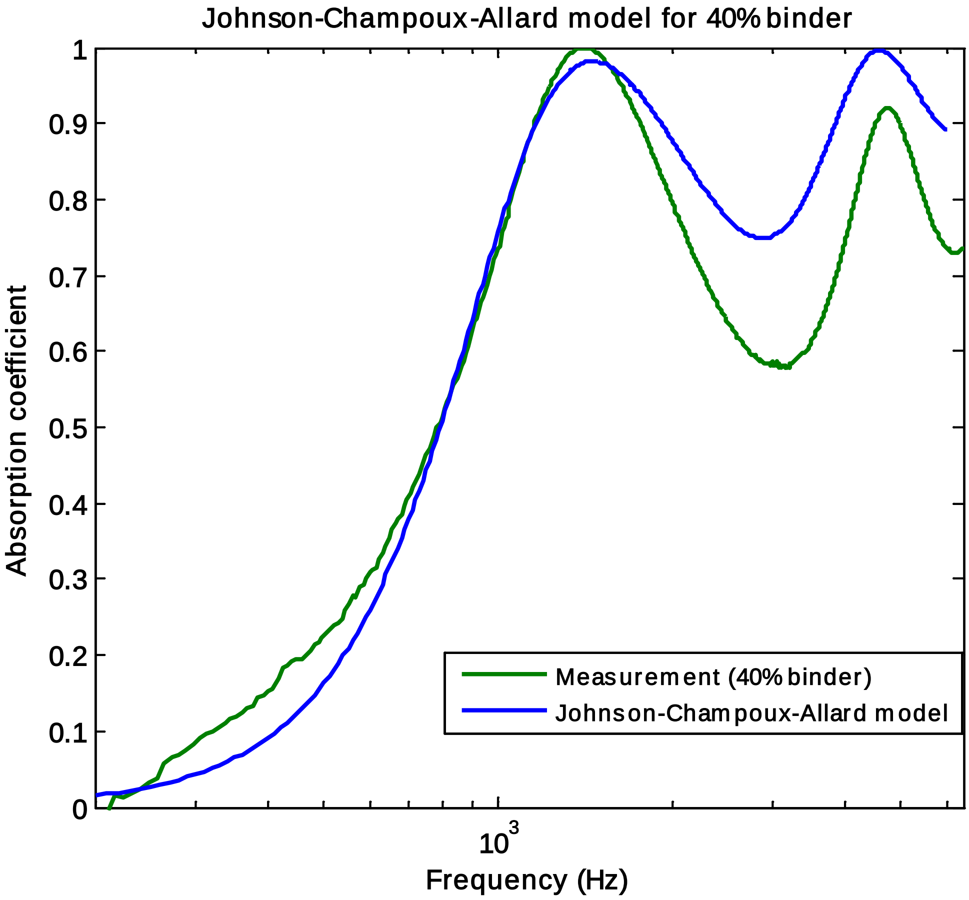

Figure 6.9: Johnson-Champoux-Allard model for 40% binder level

Table 6.10: Summary of the parameters used in the Johnson-Champoux-Allard model for 40% binder

Material	Binder (%)	Resistivity (N.s/m^4)	Porosity (%)	Tortuosity	Λ (μm)	Λ' (μm)	Thickness (mm)
Rayon(original)	40	8,600	77	1.7	-	-	32
Rayon(adjusted)	40	8,750(2%)	80(4%)	1.8(6%)	60	15	32(0%)

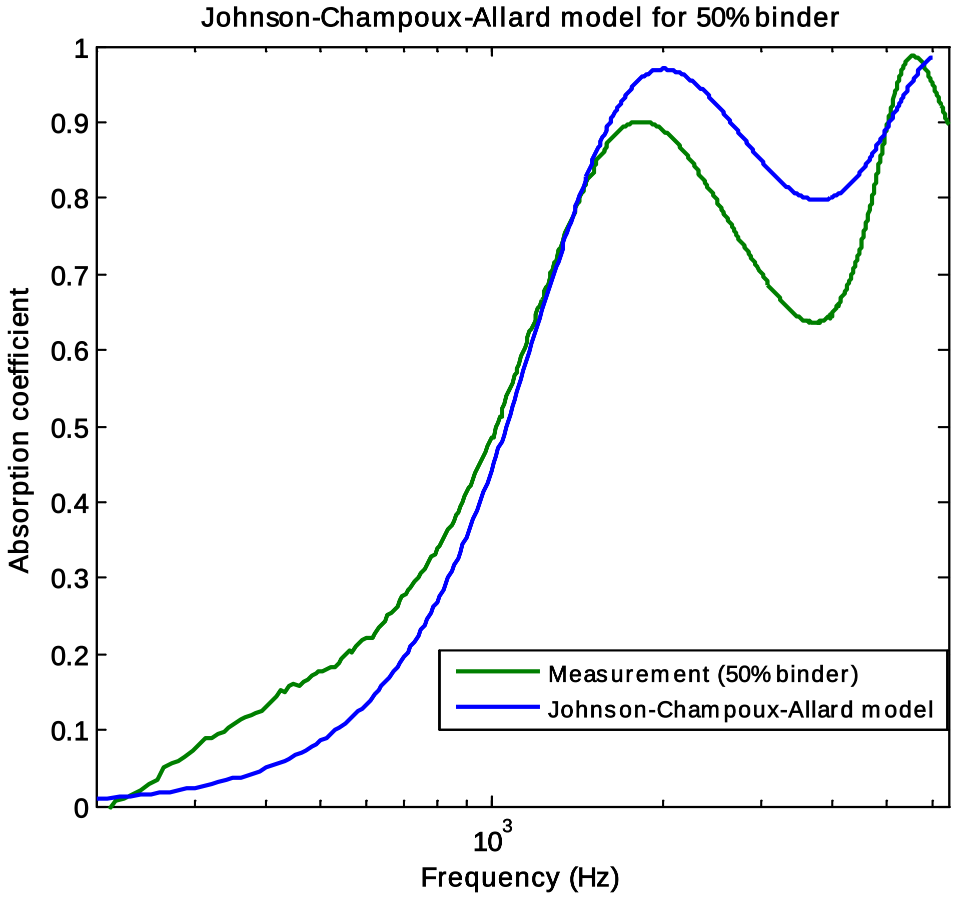

Figure 6.10: Johnson-Champoux-Allard model for 50% binder level

Table 6.11: Summary of the parameters used in the Johnson-Champoux-Allard model for 50% binder

Material	Binder (%)	Resistivity (N.s/m^4)	Porosity (%)	Tortuosity	Λ (μm)	Λ' (μm)	Thickness (mm)
Rayon(original)	50	8,050	89.6	1.7	-	-	32
Rayon(adjusted)	50	8,750(2%)	80(4%)	1.8(6%)	65	55	32(0%)

The comparison between the experimental results and predictions show that the models can provide an agreement with the experimental results for the samples made using the cold extrusion process. Overall the Pade approximation offers a very close agreement with the measured data for the absorption coefficient of the developed materials. The

Johnson-Champoux-Allard model appears less suitable for the prediction of the acoustical properties of these materials especially at the higher binder levels. This is likely to relate to the highly heterogeneous nature and broad pore size distribution encountered in the extruded media. The tested models were sensitive to the measured values of the non-acoustic parameters, which have been used in the calculations. To improve the agreement with experimental results, these parameters can be adjusted, in some cases small parameter variations can result in an excellent agreement; although in some cases flow resistivity requires considerable adjustment.

6.4 Summary

The acoustic properties rely on the pore structure of the material. The physical manipulation of this property can be used to alter the acoustic absorption characteristics to suit particular applications. In its simplest form, the manufacture of acoustic materials requires solid granules and fibres to be mixed with a small quantity of liquid binder and subsequently compacted and pressed into shape before final curing. These structures can be modelled and optimised in relation to sound absorption and vibration transmission.

It has been proved that acoustically viable materials can be produced using the novel cold extrusion process; also the properties of these materials can be suitably controlled by varying the process parameters. The acoustical properties of the developed materials have been studied and it is recommended to scale up the extrusion process. It has been shown that the acoustical absorption performance of these materials can be modelled using a suitable theoretical basis. A very good agreement has been achieved between the measured data and the prediction obtained using the Pade approximation model in which a majority of the non-acoustical parameters have been measured.